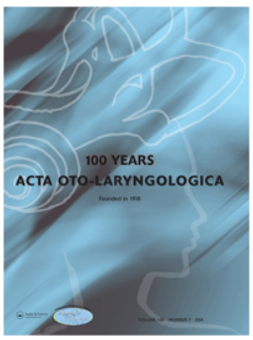

Acta Oto-Laryngologica

ISSN: 0001-6489 (Print) 1651-2251 (Online) Journal homepage: https://www.tandfonline.com/loi/ioto20

Estimation of the status of spiral ganglion neurons and Schwann cells in the auditory neural degeneration mouse using the auditory brainstem response

Zhi-Jian Zhang, Hong-Xia Guan, Kun Yang, Bo-Kui Xiao, Hua Liao, Yang Jiang, Tao Zhou & Qing-Quan Hua

To cite this article: Zhi-Jian Zhang, Hong-Xia Guan, Kun Yang, Bo-Kui Xiao, Hua Liao, Yang Jiang, Tao Zhou & Qing-Quan Hua (2018) Estimation of the status of spiral ganglion neurons and Schwann cells in the auditory neural degeneration mouse using the auditory brainstem response, Acta Oto-Laryngologica, 138:7, 603-609, DOI: 10.1080/00016489.2018.1436766

To link to this article: https://doi.org/10.1080/00016489.2018.1436766

Published online: 19 Mar 2018.

ACTA OTO-LARYNGOLOGICA, 2018
VOL. 138, NO. 7, 603–609
https://doi.org/10.1080/00016489.2018.1436766

Taylor & Francis
Taylor & Francis Group

RESEARCH ARTICLE

Estimation of the status of spiral ganglion neurons and Schwann cells in the auditory neural degeneration mouse using the auditory brainstem response

Zhi-Jian Zhang[a]*, Hong-Xia Guan[b]*, Kun Yang[a], Bo-Kui Xiao[a], Hua Liao[a], Yang Jiang[a], Tao Zhou[a] and Qing-Quan Hua[a]

[a]Department of Otolaryngology – Head and Neck Surgery, Renmin Hospital of Wuhan University, Wuhan, China; [b]Department of Otolaryngology – Head and Neck Surgery, Hubei Maternal and Child Health Hospital, Wuhan, China

ABSTRACT

Conclusion: The auditory brainstem response (ABR) wave I threshold, latency and amplitude are insensitive to spiral ganglion neurons (SGNs) degeneration, but are sensitive to the degeneration of Schwann cells and can estimate the status of Schwann cells in a neural degeneration mouse model. The thorough pre-operative ABR assessment would be helpful in predicting cochlear implant performance.

Objectives: This study aimed in finding a non-invasive electrophysiological method to evaluate the status of the auditory nerve and the Schwann cells in sensorineural hearing loss (SNHL) and auditory neuropathy (AN) ears, and providing useful information for candidates screening and outcome prediction in cochlear implantation.

Methods: The frequency-specific acoustic ABR was recorded in mice. The immunohistochemical staining was performed to detect the SGNs and Schwann cells in mice cochlea. The correlations between ABR wave I metrics and SGNs, Schwann cells were investigated.

Results: In SNHL and AN mice cochlea, statistically significant correlations between ABR wave I thresholds, latencies and amplitudes at 8, 16, and 32 kHz and their corresponding SGNs densities were found only in wave I amplitude at 8 kHz. While the ABR wave I metrics at all three frequencies showed strong significant correlations with their corresponding Schwann cells densities.

ARTICLE HISTORY
Received 21 October 2017
Revised 26 December 2017
Accepted 9 January 2018

KEYWORDS
Auditory brainstem response; spiral ganglion neurons; Schwann cells; sensorineural hearing loss; cochlear implant; mouse

Introduction

Sensorineural hearing loss (SNHL), which results from pathologies of the cochlea and the auditory nerve, is a common communication disorder. Loss of inner ear hair cells and degeneration of spiral ganglion neurons (SGNs) in the cochlea are the typical causes for SNHL. Currently, gene therapy or stem cell replacement therapy is not yet available, cochlear implantation is the best hearing rehabilitation strategy for severe-to-profound SNHL and auditory neuropathy (AN) patients. Cochlear implants (CIs) bypass the lost hair cells and directly stimulate SGNs, of which the axons form the auditory nerve. Proper functioning of CIs hence mainly depends on the existence of sufficient and functional auditory neuronal structures especially the SGNs in the deafened ears, and the status of these remnant neural structures likely directly impacts cochlear implant outcomes [1–3]. SGNs are bipolar neurons that are enwrapped by Schwann cells in the cochlea Rosenthal's canal. Schwann cells play important roles in providing myelin layers, as well as in energy conservation, neurotrophin support, and in promoting SGNs health and survival [4–7], contribute to an important part as the status of the auditory neuronal structures, therefore, are worthy of detailed investigation.

For the assessment of the auditory nerve's state, the electrically evoked compound action potential (ECAP) and auditory brainstem response (EABR) have been used [8,9]. However, the recording method requires surgical exposure of the round window thus precluding pre-operative applications in routine clinical settings [2].

The acoustic auditory brainstem response (ABR) is an evoked potential recorded non-invasively from the scalp that reflect synchronous neural activity within the auditory nerve, subsequent fiber tracts, and nuclei within the auditory brainstem pathways. The threshold, amplitude, and latency analysis of the ABR can provide a rapid assessment on the peripheral hearing status and the integrity of brainstem pathways, thus, ABR is widely used in both clinical and research settings. Taking the advantages of the merits of ABR as above and a well-established animal model for SNHL and AN [10], we investigated the relationships between ABR metrics and SGNs and Schwann cells in the cochlea Rosenthal's canal aiming in finding a non-invasive electrophysiological method to evaluate the status of the auditory neuronal structures in SNHL and AN ears. The results from this study may provide important information for pre-operative evaluating the outcomes in CI recipients.

CONTACT Zhi-Jian Zhang 2976160748@qq.com Department of Otolaryngology-Head and Neck Surgery, Renmin Hospital of Wuhan University, 238 Jie-Fang Road, Wuhan 430060, China; Qing-Quan Hua hqqrm@sina.com Department of Otolaryngology-Head and Neck Surgery, Renmin Hospital of Wuhan University, 238 Jie-Fang Road, Wuhan 430060, China
*These authors have equally contributed to this work.

Materials and methods

Animals

Experiments were performed on adult female CBA/CaJ mice, aged 8–12 weeks. All mice were kept under standard laboratory conditions, received food and water and were maintained on a 12-h light/dark cycle. One group served as normal controls ($n = 8$), while the other 24 mice were exposed to ototoxic treatment and used as experimental group. All surgical and experimental procedures in this study were approved by the local Animal Care and Use Committee.

Surgical procedures

The auditory neural degenerations were accomplished by application of 0.5mM ($n = 8$), 1 mM ($n = 8$) and 3mM ($n = 8$) ouabain (Sigma-Aldrich, St. Louis, MO) to the round window niche, as described previously [10]. Briefly, the animal was anesthetized by an intraperitoneal injection of sodium pentobarbital (50 mg/kg) and placed in a heating pad to maintain its body temperature. Under the microscope, the right bulla was exposed via a post-auricular approach, a small perforation was made to further expose the round window niche. Using microinjection, 10 µl saline (for mice in control group) or same volume of ouabain (for mice in experimental group) was directly applied to the intact round window with a total 60 min of ouabain exposure time.

The auditory brainstem response (ABR)

The ABR testing was performed by using TDT BioSig III system (Tucker Davis Technologies, Alachua, FL) in a sound isolation chamber. Following anesthesia as above, responses were recorded using subcutaneous needle electrodes placed at the vertex, below the pinna of the right ear (reference), and below the contralateral ear which was blocked with a sound-attenuating earplug (ground). ABRs were measured in response to tone pips of 8, 16 and 32 kHz with 5 ms duration and a 0.5 ms rise-fall time. Signal recordings in response to tone pips were amplified and averaged 1000 times. Tone pips were presented at 80 dB SPL and decreased in 10 dB SPL increments until ABR wave I was no longer visually identifiable, and then increased by 5 dB SPL to define the hearing threshold. ABR wave I latencies and amplitude stimulated by 80 dB SPL tone pips were recorded.

Cochlea section immunohistochemistry

Thirty days after saline or ouabain exposure, after the ABRs assessments, the anesthetized mice were sacrificed and their cochleae were dissected and fixed in 4% paraformaldehyde in PBS (pH =7.4) overnight at 4 °C. After fixation, cochleae were rinsed with PBS and immersed in 10% ethylenediaminetetraacetic acid (EDTA) at 4 °C for decalcification. Then they were incubated overnight in 30% sucrose for cryoprotection, embedded in O.C.T. Tissue Tek Compound (Miles Scientific, Newark, DE), cryosectioned parallel to the modiolar at 10 µm thickness, mounted and stored at −20 °C until use.

The double immunofluorescent staining was same as described previously [10]. In brief, mice mid-modiolar frozen sections were incubated overnight at 4 °C with the primary antibodies: mouse anti-βIII tubulin (1:500; ab78078; Abcam, Cambridge, MA), and rabbit anti-S-100β (1:500; ab52642; Abcam, Cambridge, MA), which marked SGNs and Schwann cells in the Rosenthal's canal, respectively. The sections were washed three times in PBS and were incubated with the corresponding secondary antibodies (Alexa Fluor 488 or 594, Invitrogen, Carlsbad, CA) at room temperature for 1 h. Following the removal of the secondary antibodies and before the final washes, the sections were exposed for 15 min at room temperature to a fluorescent dye 4′,6′-diamidino-2-phenylindole dihydrochloride (DAPI; Sigma-Aldrich, St. Louis, MO). The sections were rinsed in PBS and mounted in an antifade medium. The immunolabeled sections were examined and the images were acquired using a fluorescence microscope (Olympus BX53, Tokyo, Japan). To quantify immuno-positive SGNs and Schwann cells in the

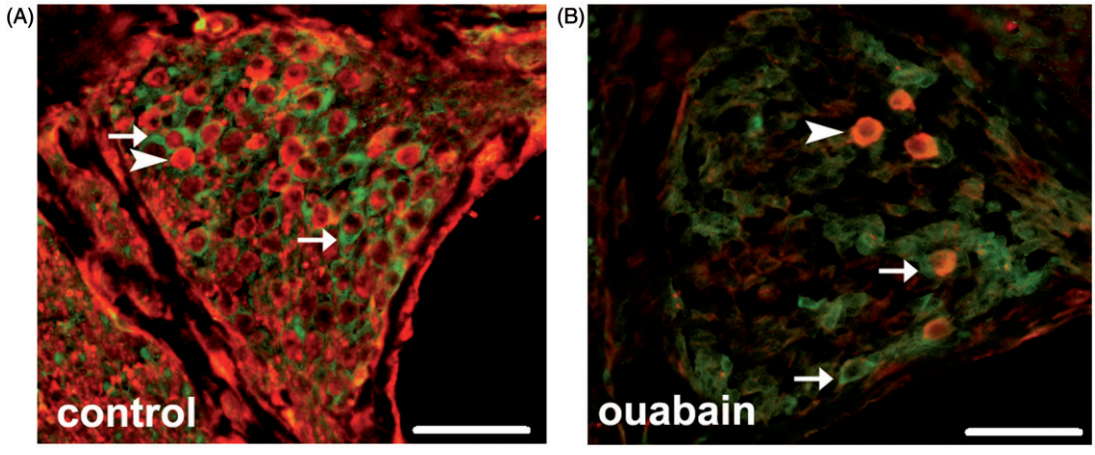

Figure 1. Double immunostaining of SGNs (β-III tubulin; arrowheads) and cochlea Schwann cells (S-100β; arrows) in Rosenthal's canal in a middle turn in control mice (A) and in ouabain-treated mice (B), 30 d after ouabain exposure, the numbers of β-III tubulin-positive cells, and S-100β-positive cells were significantly decreased (B). The scale bar represents 50 µm.

Rosenthal's canal from apical, middle and basal turns, ImageJ software (NIH Image J system, Bethesda, MD) was used, and Abercromie correction factors were applied for cell counting.

Statistical analysis

All data values were presented as the mean with standard error mean (SEM). Statistical analysis was performed with Prism 5.0 software (GraphPad Software, La Jolla, CA). Student's *t*-test was used for group comparisons. Linear regression was used for correlation analyses, and false discovery rate correction was used in the multiple testing. Significant statistical differences were considered at $p < .05$ level.

Results

Immunohistochemistry

Immunostaining in mid-modiolar sections from the middle turns of the control and ouabain-treated groups is shown in Figure 1, which was same as the results we previously described [10]. Beta III tubulin was used as a marker for both type I and type II SGNs, and S-100β was used to mark Schwann cells in mouse cochleae. In the control group, the profile and the density of SGNs in Rosenthal's canal were all within the normal range, the perikaryons of the majority of neurons were surrounded by Schwann cells labeled by S-100β (Figure 1(A)). While in the ouabain-treated group, extensive significant damage of SGNs and Schwann cells was observed, and the surviving cells were obviously

Table 1. Comparisons of ABRs, SGNs, and Schwann cells between control and ouabain-treated groups.

	8 kHz		16 kHz		32 kHz	
	Control	Ouabain	Control	Ouabain	Control	Ouabain
Threshold (dBSPL)	57.5 ± 2.8	61.3 ± 2.0	36.9 ± 2.7	53.8 ± 2.7**	33.8 ± 3.2	50.4 ± 2.4***
Latency (ms)	1.47 ± 0.08	1.88 ± 0.06**	1.34 ± 0.11	1.79 ± 0.06***	1.36 ± 0.07	1.73 ± 0.06**
Amplitude (μV)	1.21 ± 0.1	0.39 ± 0.05***	1.46 ± 0.12	0.5 ± 0.06***	1.64 ± 0.12	0.5 ± 0.06***
SGNs (cells/mm^2)	1672.3 ± 19.8	206.2 ± 17.9***	1736.3 ± 60.5	227.7 ± 21.7***	1702.5 ± 49.9	215.8 ± 19.6***
Schwann cells (cells/mm^2)	3879.5 ± 107.1	2734.8 ± 111.8***	3842.3 ± 175.4	2660.3 ± 120.9***	3781.1 ± 179.8	2742.9 ± 97.4***

Control: $n = 8$; ouabain: $n = 24$. ** $p < .01$; *** $p < .001$.

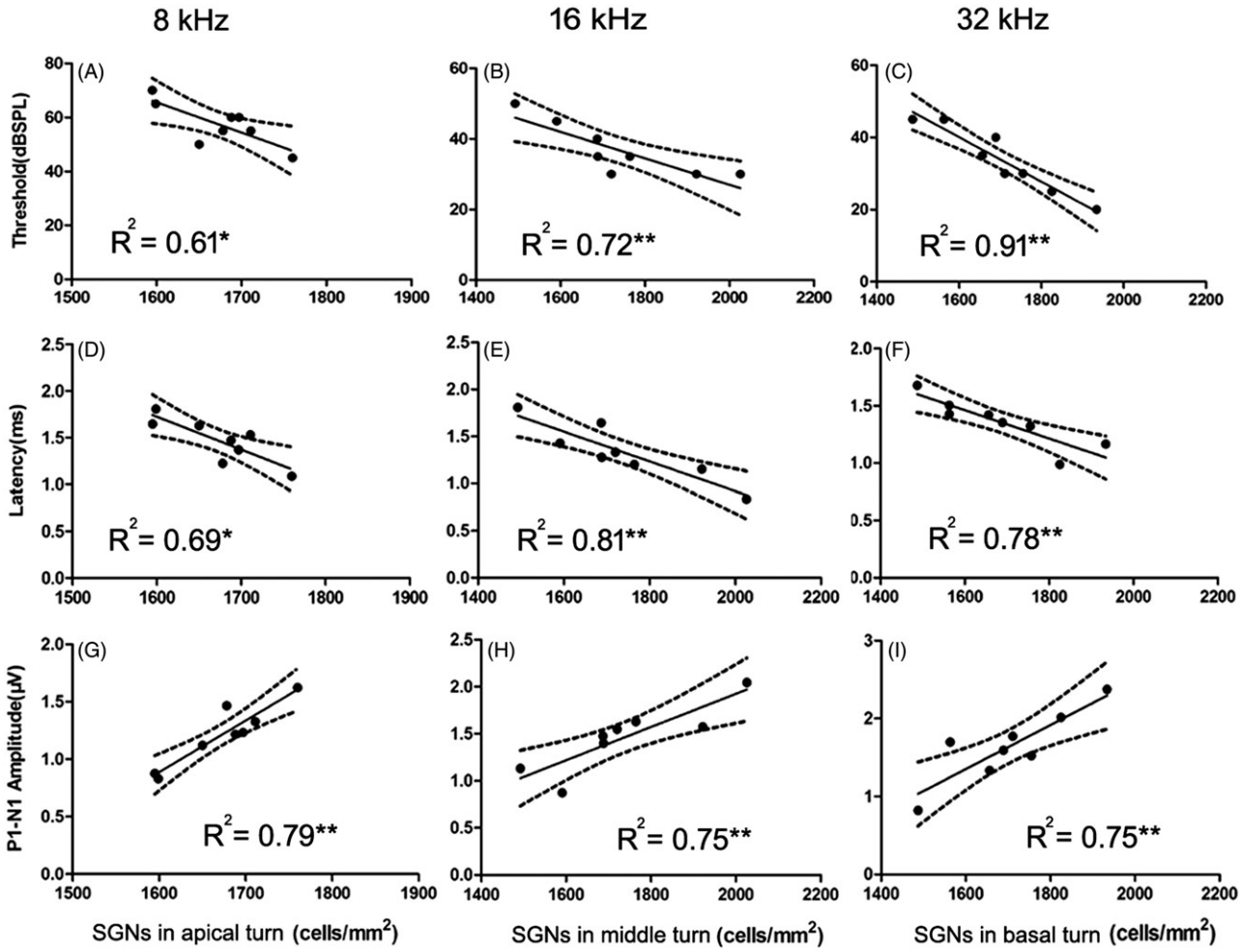

Figure 2. The correlations between the ABR metrics at 8, 16, and 32 kHz and the densities of the spiral ganglion neurons (SGNs) from the apical, middle, and basal turns, respectively, in normal mice ($n = 8$). (A), (B), and (C) ABR thresholds; (D), (E), and (F) wave I latencies; (G), (H), and (I) wave I amplitudes. Solid lines are regression lines with SGNs density as independent variate. *$p < .05$; **$p < .01$.

disorganized (Figure 1(B)). Similar results were also found in the apical and basal turns (data not shown). The cell counting results revealed that the cell densities of SGNs and Schwann cells in apical, middle and basal turns in the ouabain-treated group were significantly decreased compared with those in the control group (Table 1).

ABR

Mean ABR thresholds, wave I latencies, and amplitudes at 8, 16 and 32 kHz for the control and the ouabain-treated group are shown in Table 1. ABR thresholds at 16 and 32 kHz in the ouabain group were significantly elevated compared with the control group. Furthermore, a significant increase in wave I latencies was seen at 8, 16, and 32 kHz in ouabain-treated mice, as compared with the control mice. Amplitudes of wave I were measured as the difference between the positive peak and the following negative trough in this study. As shown in Table 1, the ABR wave I amplitudes at 8, 16, and 32 kHz from the ouabain-treated mice were significantly decreased compared with those of the control mice.

Correlations between SGNs density and ABR metrics

Due to the cochlear tonotopicity, in this study, frequency-specific ABRs were recorded to examine the cochlea functions from the related cochlea regions. Three frequencies of 8, 16, and 32 kHz are corresponding to the apical, middle, and basal turns of the cochlea, respectively [11], therefore, were classically tested in this study.

The correlations between the ABR metrics (wave I threshold, latency and amplitude) and the SGNs density in corresponding cochlea region in control mice are shown in Figure 2. The results revealed that the ABR thresholds at all 3 frequencies of 8, 16, and 32 kHz significantly decreased with the increase of their corresponding SGNs densities, respectively (Figure 2(A–C)). Similarly, a significant negative correlation between the ABR wave I latency and the corresponding SGNs density was found (Figure 2(D–F)). For the ABR wave I amplitudes at all three frequencies and their corresponding SGNs densities, a significant positive correlation was observed between them (Figure 2(G–I)).

Figure 3 shows the relationships between the ABR metrics (wave I threshold, latency, and amplitude) and the SGNs density in corresponding cochlea region in ouabain mice. The ABR thresholds at 8, 16, and 32 kHz were not

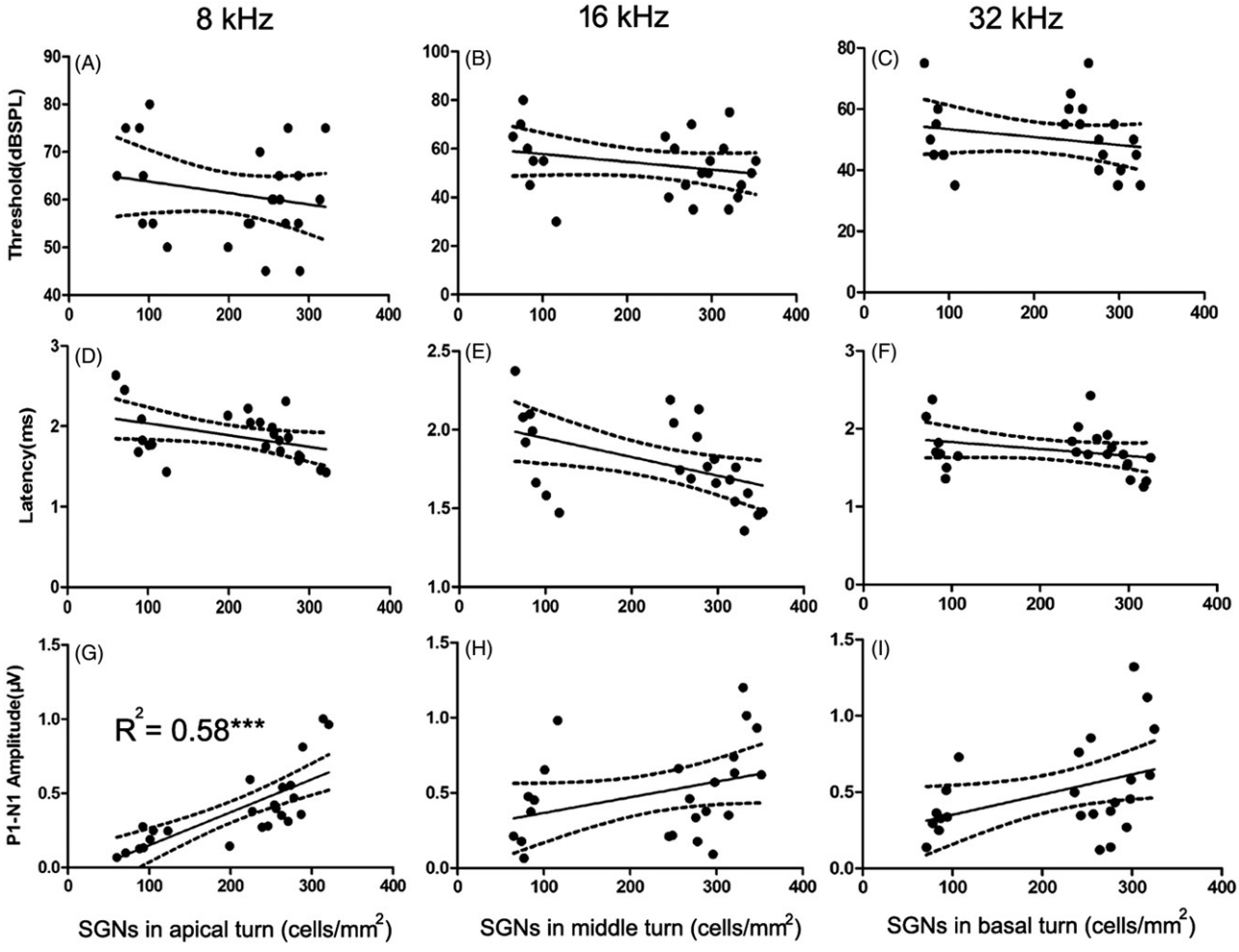

Figure 3. The correlations between the ABR metrics at 8, 16, and 32 kHz and the densities of the spiral ganglion neurons (SGNs) from the apical, middle, and basal turns, respectively, in ouabain-treated mice ($n = 24$). (A), (B), and (C) ABR thresholds; (D), (E), and (F) wave I latencies; (G), (H), and (I) wave I amplitudes. Solid lines are regression lines with SGNs density as independent variate. $^{***}p < .001$.

associated with the SGNs densities in the apical, middle, and basal turns of the cochlea, respectively (Figure 3(A–C)). The ABR wave I latencies at 8 and 16 kHz but not 32 kHz showed negative correlations with the SGNs densities, nevertheless, the differences were no longer significant after false discovery rate correction (Figure 3(D–F)). Significant positive correlation between the SGNs density and the ABR wave I amplitude was observed only at 8 kHz but not at 16 and 32 kHz (Figure 3(G–I)).

Correlations between Schwann cells density and ABR metrics

The relationships between the ABR metrics (wave I threshold, latency, and amplitude) and the Schwann cells density in control cochlea were also investigated, and the results are shown in Figure 4. The ABR thresholds at 8, 16, and 32 kHz were statistically associated with the SGNs densities from the apical, middle, and basal turns in the cochlea, respectively (Figure 4(A–C)). Similarly, a significant negative correlation between the ABR wave I latency and the corresponding Schwann cells density was obtained (Figure 4(D–F)). Moreover, the ABR wave I amplitudes at all three frequencies also showed significant correlations with the corresponding Schwann cells densities (Figure 4(G–I)).

Figure 5 illustrates the correlations between the ABR metrics and the Schwann cells density in ouabain-treated cochlea. The results in Figure 5 are similar to those shown in Figure 4. Overall, the ABR thresholds, wave I latencies and amplitudes at 8, 16, and 32 kHz all presented statistically significant correlations with the corresponding Schwann cells densities (Figure 5).

Discussion

The ABR reveals the electrical responses of both the auditory nerve and the nuclei of the central auditory pathway to sound stimulation. The ABR pattern of mice typically contains five identifiable wave forms labeled as I–V [12]. It is generally considered that wave I represents the activities from the SGNs and the auditory nerve while the later waves represent neural responses from the ascending auditory

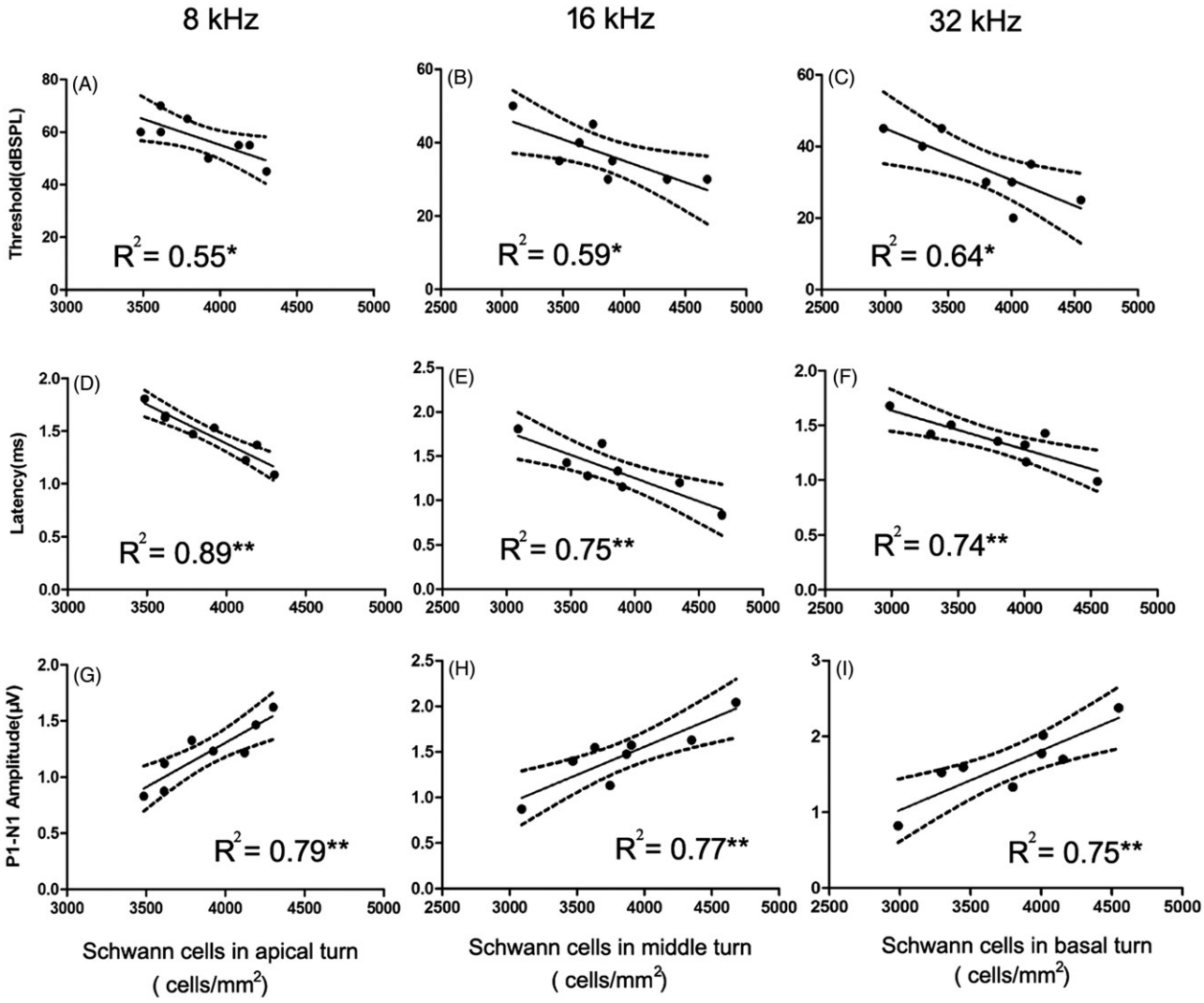

Figure 4. The correlations between the ABR metrics at 8, 16, and 32 kHz and the densities of the Schwann cells densities from the apical, middle, and basal turns, respectively, in normal mice ($n = 8$). (A), (B), and (C) ABR thresholds; (D), (E), and (F) wave I latencies; (G), (H), (I) wave I amplitudes. Solid lines are regression lines with Schwann cells density as independent variate. $^{*}p < .05$; $^{**}p < .01$.

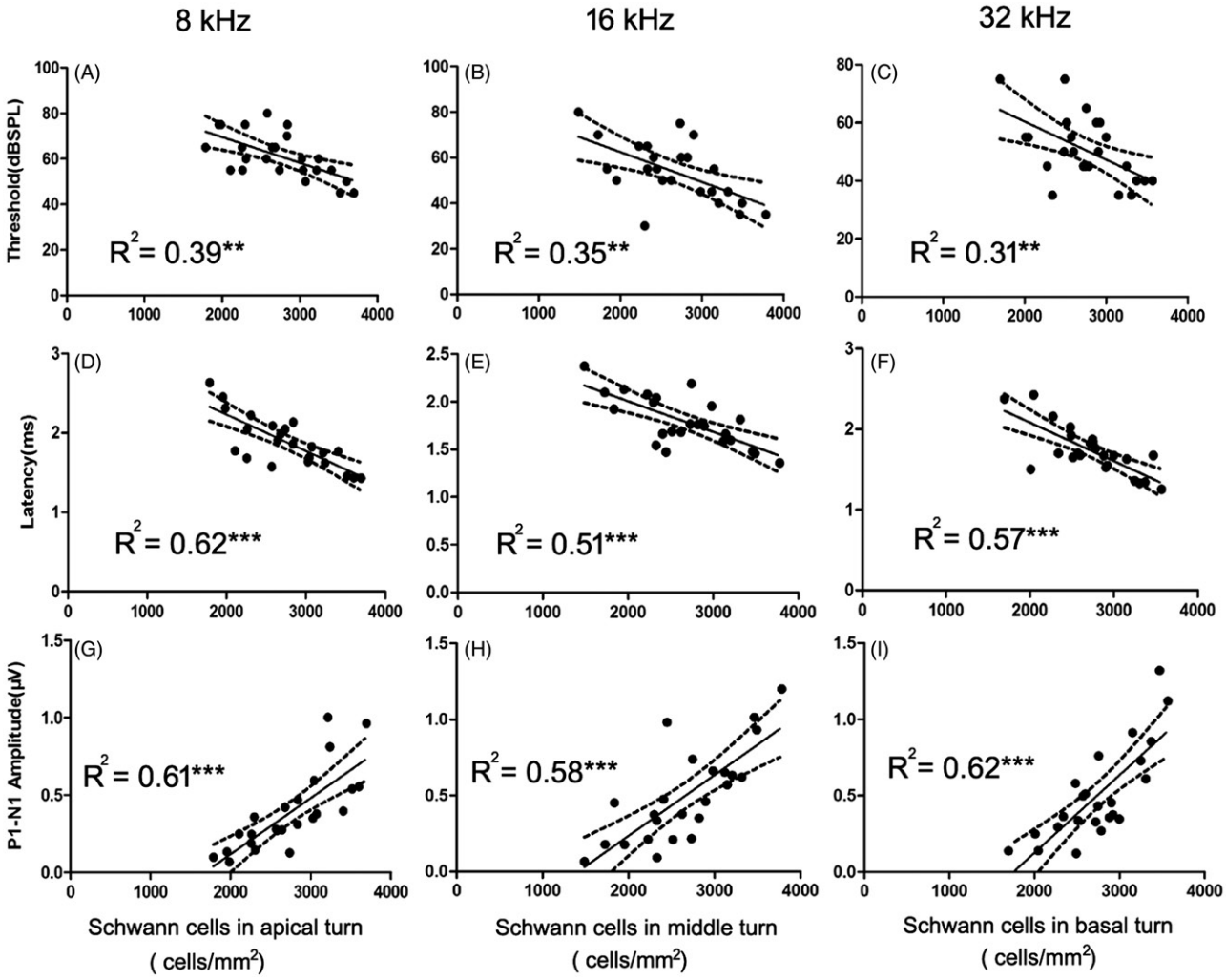

Figure 5. The correlations between the ABR metrics at 8, 16, and 32 kHz and the densities of the Schwann cells densities from the apical, middle, and basal turns, respectively, in ouabain-treated mice ($n = 24$). (A), (B), and (C) ABR thresholds; (D), (E), and (F) wave I latencies; (G), (H), and (I) wave I amplitudes. Solid lines are regression lines with Schwann cells density as independent variate. $^{**}p < .01$; $^{***}p < .001$.

pathway in mice. We have successfully recorded frequency-specific ABRs from CBA/CaJ mice in this study. Since the SGNs and the auditory nerve are our concerns, we have specifically examined the amplitude, the latency as well as the threshold of ABR wave I. As shown in Figures 2 and 4, in normal cochlear apical, middle, and basal turns, strong significant correlations were observed among the SGNs, the Schwann cells, and their corresponding ABR thresholds, latencies, and amplitudes, respectively. Our findings suggest that sufficient amounts of the SGNs and the Schwann cells with good quality are essential for normal electrophysiological functions of the auditory nerve, and ABR can be a useful tool to assess the status of the SGNs and the Schwann cells under normal condition.

In the present study, we used our previously established SNHL and AN model [10] to study the relationships between ABR and the SGNs and the Schwann cells under cochlea neural degeneration (with intact hair cells) condition. Similar to the previous studies [13,14], significant degenerations of the SGNs, the Schwann cells as well as elevated ABR wave I thresholds (except for 8 kHz), increased latencies of wave I and decreased amplitudes of wave I were found in the ouabain-treated cochlea (Figure 1 and Table 1). Under this cochlea neural degeneration condition, the significant correlations between the SGNs and their corresponding ABR wave I thresholds, latencies, and amplitudes under normal condition were almost lost (Figures 2 and 3). The results indicated that ABR wave I thresholds, latencies, and amplitudes were insensitive to the even very remarkable degenerations of SGNs since there were only about 12–13% SGNs survived in ouabain-treated cochlea compared with normal cochlea (Table 1). One explanation for the insensitivity of the ABR wave I metrics to SGNs damage is that the possible hype-function of the surviving SGNs, since the hair cells were intact, the high degree of divergence from each intact inner hair cell to multiple surviving afferent nerve fibers together with the possible support from the surviving Schwann cells may make the surviving SGNs hype-functional, nevertheless, the precise mechanisms need to be further investigated. Regardless of the underlying mechanism, the results have important implications for using ABR wave I metrics to monitor the SGNs degeneration when hair cells are intact, the ABR testing results should be interpreted cautiously to avoid underestimating the SGNs damage. More sensitive measures of the state of SGNs are needed for experimental and clinical use.

The bipolar SGNs make up the auditory nerve, the peripheral portion of the auditory nerve is surrounded by myelinating Schwann cells (for type I SGNs), and non-myelinating Schwann cells (for type II SGNs). Schwann cells play important roles in neural survival and for normal electrophysiological functions of the SGNs [4–7], and may directly affect the SGNs, thus we particularly studied the Schwann cells as a part of the state of the auditory nerve in this study. We found that about 69–73% of Schwann cells survived after ouabain treatment compared with that in normal mice (Table 1). The relative higher survival of the Schwann cells over the SGNs (12–13%) after ouabain treatment may because that the SGNs death resulted from the blockage of the α3 subunit of the Na+/K + ATPase by ouabain, this α3 subunit predominated in the SGNs but not the Schwann cells in mouse cochlea [15]. Our previous study showed that ouabain damaged the Schwann cells in a dose- and time-dependent manner [10]. In addition, our recent results demonstrated that the surviving Schwann cells significantly correlated with the surviving SGNs at 30 d after ouabain treatment (data not shown). Thus we speculate that two possible mechanisms involved in the death of the Schwann cells, those are the directly apoptotic death triggered by high dosage (3 mM) of ouabain and the degeneration secondary to the loss of SGNs.

In ouabain-treated cochlea, the surviving Schwann cells sustained the strong significant correlations with their corresponding ABR metrics which were observed in normal control cochlear (Figures 4 and 5), therefore, ABR wave I thresholds, wave I latencies, and amplitudes can be used to evaluate the state of the Schwann cells even under neural degeneration conditions.

In summary, the present study demonstrates that ABR wave I thresholds, wave I latencies, and amplitudes are sensitive to the degeneration of the Schwann cells, however, are insensitive to the degeneration of the SGNs in a SNHL and AN mouse model. Therefore, our findings suggest that preoperative measurement of the ABR in the SNHL especially in the auditory neuropathy patients, in addition to its usual roles, could provide important information about the status of the Schwann cells, which could be useful in candidates screening and outcome prediction for cochlear implantations. Since ABR wave I metrics are insensitive for the SGNs evaluation, the ABR testing results should be interpreted cautiously to avoid misjudging the SGNs damage, and more sensitive measures of the state of SGNs are desired for experimental and clinical use.

Disclosure statement

The authors report no conflicts of interest. The authors alone are responsible for the content and writing of the paper.

Funding

This work was supported by the National Natural Science Foundation of China and China Education Ministry Scientific Research Foundation for the Returned Overseas Scholars.

References

[1] Blamey P, Artieres F, Başkent D, et al. Factors affecting auditory performance of postlinguistically deaf adults using cochlear implants: an update with 2251 patients. Audiol Neurotol. 2013;18:36–47.

[2] McClellan JH, Formeister EJ, Merwin WH 3rd, et al. Round window electrocochleography and speech perception outcomes in adult cochlear implant subjects: comparison with audiometric and biographical information. Otol Neurotol. 2014;35: e245–e252.

[3] Rance G, Starr A. Pathophysiological mechanisms and functional hearing consequences of auditory neuropathy. Brain. 2015;138:3141–3158.

[4] Hansen MR, Vijapurkar U, Koland JG, et al. Reciprocal signaling between spiral ganglion neurons and Schwann cells involves neuregulin and neurotrophins. Hear Res. 2001;161: 87–98.

[5] Tang W, Zhang Y, Chang Q, et al. Connexin29 is highly expressed in cochlear Schwann cells, and it is required for the normal development and function of the auditory nerve of mice. J Neurosci. 2006;26:1991–1999.

[6] Pettingill LN, Minter RL, Shepherd RK. Schwann cells genetically modified to express neurotrophins promote spiral ganglion neuron survival in vitro. Neuroscience. 2008;152: 821–828.

[7] Zhou R, Assouline JG, Abbas PJ, et al. Anatomical and physiological measures of auditory system in mice with peripheral myelin deficiency. Hear Res. 1995;88:87–97.

[8] Hall RD. Estimation of surviving spiral ganglion cells in the deaf rat using the electrically evoked auditory brainstem response. Hear Res. 1990;49:155–168.

[9] Ramekers D, Versnel H, Strahl SB, et al. Auditory-nerve responses to varied inter-phase gap and phase duration of the electric pulse stimulus as predictors for neuronal degeneration. Jaro. 2014;15:187–202.

[10] Zhang ZJ, Guan HX, Yang K, et al. Dose-dependent effects of ouabain on spiral ganglion neurons and Schwann cells in mouse cochlea. Acta Otolaryngol. 2017;137:1017–1023.

[11] Müller M, von Hünerbein K, Hoidis S, et al. A physiological place-frequency map of the cochlea in the CBA/J mouse. Hear Res. 2005;202:63–73.

[12] Zhou X, Jen PH, Seburn KL, et al. Auditory brainstem responses in 10 inbred strains of mice. Brain Res. 2006; 1091:16–26.

[13] Yuan Y, Shi F, Yin Y, et al. Ouabain-induced cochlear nerve degeneration: synaptic loss and plasticity in a mouse model of auditory neuropathy. Jaro. 2014;15:31–43.

[14] Lang H, Li M, Kilpatrick LA, et al. Sox2 up-regulation and glial cell proliferation following degeneration of spiral ganglion neurons in the adult mouse inner ear. Jaro. 2011;12:151–171.

[15] Erichsen S, Zuo J, Curtis L, et al. Na,K-ATPase alpha- and beta-isoforms in the developing cochlea of the mouse. Hear Res. 1996;100:143–149.